

Note: Snapshot PDF is the proof copy of corrections marked in EditGenie, the layout would be different from typeset PDF and EditGenie editing view.

## Author Queries & Comments:

**Q1 :** The distinction between surnames can be ambiguous, therefore to ensure accurate tagging for indexing purposes online (e.g. for PubMed entries), please check that the highlighted surnames have been correctly identified, that all names are in the correct order and spelt correctly.

**Response:** Surnames are fine.

**Q2 :** Please note that tables cannot be reproduced in color due to journal style. Please consider an alternative format (ex: using bold font, italics, etc. to make the distinctions).

**Response:** Sample numbers changed according to recommendation. Please, remove gray shading in Tables 1, 2 and 3.

**Q3 :** The year is mentioned as "1985" for Reference Aitken in text whereas in Ref list as "1998". Please check and clarify which one is correct.

**Response:** Reference changed in the Reference section. 1985 is correct.

**Q4 :** The Duller, 2015 is cited in text, whereas it is not listed in References. Please list or delete the citation.

**Response:** Duller is wrong. Durcan et al. is correct.

### Color coding for Comments and editing changes:

1. <b>Author</b>	(a) <b>Text insertion;</b> (b) <b>Text Deletion;</b> (c) <b>Text Formatting;</b> (d) <b>Text Comments</b>
2. <b>Editor</b>	All track changes and comments.
3. <b>Assitant Editor</b>	All track changes and comments.
4. <b>Associate Editor</b>	All track changes and comments.
5. <b>Forum Editor</b>	All track changes and comments.
6. <b>Production editor</b>	All track changes and comments.
7. <b>Copyeditor</b>	All track changes and comments.
8. <b>Proofreader</b>	All track changes and comments.
9. <b>Managing editor</b>	All track changes and comments.
10. <b>Digital review editor</b>	All track changes and comments.
11. <b>Master Copy</b>	All track changes and comments.

Heinrich Events

# Massive Deposition of Sahelian Dust on the Canary Island Lanzarote during North Atlantic Heinrich Events

**Verso running head :** Hartmut Heinrich et al

**Recto running head :** Massive Deposition of Sahelian Dust on the Canary Island Lanzarote during North Atlantic Heinrich Events

 Hartmut Heinrich<sup>a</sup>, Christoph Schmidt<sup>b</sup>, Florian Ziemer<sup>c</sup>, Uwe Mikolajewicz<sup>d</sup>, Christopher-Bastian Roettig<sup>e</sup>[Q1]

<sup>a</sup> 10°E maritime consulting, Falkenburger Ring 4, 22147 Hamburg

<sup>b</sup> University of Bayreuth and Géopolis - Office 4414, Université de Lausanne, 1015 Lausanne

<sup>c</sup> Max-Planck-Institut für Meteorologie Hamburg and Deutsches Klimarechenzentrum GmbH (DKRZ), Bundesstraße 45 a, 20146 Hamburg

<sup>d</sup> Max-Planck-Institut für Meteorologie Hamburg, Bundesstr. 53, 20146 Hamburg

<sup>e</sup> Institut für Geographie, Technische Universität Dresden, Helmholtzstraße 10, 01069 Dresden

Corresponding author at e-mail: 10e-maritime-consult@web.de (H. Heinrich)

**History :** received : 2020-04-16 accepted : 2020-09-24

**Copyright Line:** Copyright © University of Washington. Published by Cambridge University Press, 2020

## Abstract

New IRSL ages of eolianites close to Muñique (Lanzarote) demonstrate the influence of millennial scale climatic variability on the sedimentary dynamics on the Canary Islands during the last glacial cycle. The repetitive succession of interstadial and stadial climatic conditions formed multiple sequences of eolian deposits, each in general comprising three depositional types. DepoType 1 and DepoType 2 consist mainly of marine biogenic carbonate detritus with small amounts of dust from the Sahara representing interstadial conditions. DepoType 2 compared to DepoType 1 is characterized by larger amounts of land snails and calcified brood cells. A DepoType 3 rich in dust from African subtropical/tropical Latisols terminates a sequence. IRSL dating on DepoType 3 type deposits clearly shows that these were deposited during Heinrich Events under stadial conditions. The stadial cooling of the North Atlantic Ocean caused a southern shift of climate zones that culminated during Heinrich Events when the arctic climate reaches its most southerly extent. As a consequence, atmospheric changes led to massive dust supply from the then-dry Sahel. The increase in dust and precipitation from the dry DepoTypes 1 to the more humid DepoTypes 3 originates from a modified atmospheric dynamic during a millennial cycle.

## Keywords

- Eolianites
- Millennial scale climatic variability
- IRSL-dating
- Earth system modelling

## INTRODUCTION

Heinrich Events (H Events) are periods of collapses of ice sheets bordering the North Atlantic during the glacial (Ruddiman, 1977; Heinrich, 1988; Grousset et al., 1993; Andrews, 2000). Marine archives show that in these periods ice-rafted debris (IRD) was deposited throughout the North Atlantic down to about 42°–45° N (Ruddiman, 1977; Grousset et al., 1993; Andrews, 2000). Originally, during the last interglacial-glacial cycle, eleven events represented by IRD were identified in the northeast Atlantic (Chapman and Shackleton, 1998; McManus et al., 1999; Wright and Flower, 2002; de Abreu et al., 2003; Voelker and de Abreu, 2011). The most intensive events occurred during the main phase of the Weichselian/Wisconsin glaciation (Marine Oxygen Isotope Stages 4–2).

The oceanographic conditions of the glacial North Atlantic are well documented (Chapman and Shackleton, 1998; McManus et al., 1999; Wright and Flower, 2002; de Abreu et al., 2003; Voelker and de Abreu, 2011). Here, the lowest sea surface temperatures were found during H Events (McManus et al., 1994; Hemming, 2004). The sudden releases of large armadas of icebergs into the North Atlantic led not only to cooling but also to disturbances of the Atlantic Meridional Overturning Circulation (AMOC) (McManus et al., 1994; Hemming, 2004) and, as a consequence, to abrupt and massive changes in the oceanic and atmospheric climate (McManus et al., 1994; Hemming, 2004). The cold and less saline waters originating from the melting of iceberg armadas left the northern North Atlantic along the Iberian Peninsula and the northwest African coast towards the subtropical gyre passing the Canary Islands (Koopmann, 1981; Holz et al., 2004; Mulitza et al., 2008; Tjallingii et al., 2008; Naughton et al., 2009).

The strong cooling during H Events led to an expansion of the Arctic climate in the North Atlantic region far south to 39°N (Koopmann, 1981; Holz et al., 2004; Mulitza et al., 2008; Naughton et al., 2009). As a result, significant environmental changes occurred on the Iberian Peninsula and in northwest Africa (Koopmann, 1981; Holz et al., 2004; Mulitza et al., 2008; Tjallingii et al., 2008; Naughton et al., 2009). During these times this region suffered from severe droughts accompanied by an increase in wind force (Koopmann, 1981; Holz et al., 2004; Mulitza et al., 2008; Tjallingii et al., 2008; Naughton et al., 2009). The southern margin of the Sahara shifted into the present Sahel zone down to 14°N (Collins et al., 2013).

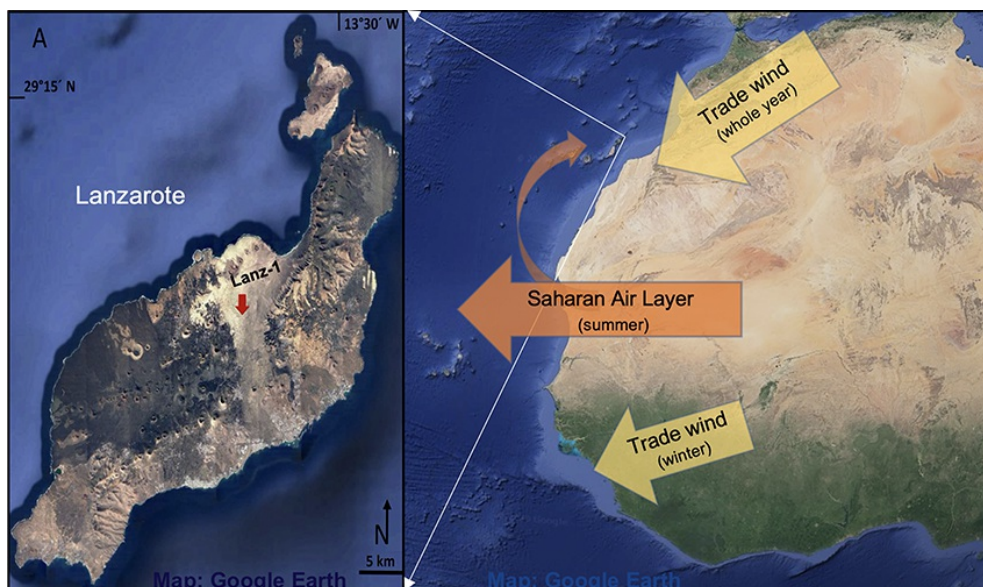
The sediment deposition on the Canary Islands, especially on Lanzarote and Fuerteventura, should therefore be strongly influenced by climate changes during the glacial periods of the Quaternary. From marine archives of the surrounding Atlantic Ocean it is known that H Events led to strong dust events (Holz et al., 2004; Jullien et al., 2007; Mulitza et al., 2008; Naughton et al., 2009; McGee et al., 2013; Williams et al., 2016; Rodrigues et al., 2017; Middleton et al., 2018). Thus, it can be expected that due to

their location in the southeastern corner of the northeast Atlantic and because of their short distance from Africa, these islands are climatically influenced by both the surrounding ocean and the nearby African continent.

The eolian deposits that cover large parts of Lanzarote and Fuerteventura are well described (Meco et al., 1997; von Suchodoletz et al., 2009; Muhs et al., 2010; Faust et al., 2015; Roettig et al., 2017; Roettig et al., 2019). The general influence of climatic processes on sedimentation has been known for a long time. However, the detailed timing of the sedimentary processes responsible for the formation of eolian dune deposits on the Eastern Canary Islands has been a matter of research for many years. Ortiz et al. (2006) presented a correlation based on amino acid racemization postulating Late Pleistocene ages of most of the sequences (Fuerteventura, Lanzarote, and the Chinijo Archipelago). Edwards and Meco (2000) and Bouab and Lamothe (1995) discussed a middle- to late Pleistocene dune formation. Until today, the most comprehensive correlation based on stratigraphic findings and luminescence dating includes different dune fields spanning from the western to the eastern coast on northern Fuerteventura (Roettig et al., 2020). Three predominant processes (deposition of carbonate sand, deposition of dust, and water-induced erosion) form a climatological cycle which in their paper is defined as a stratigraphic unit (Roettig et al., 2019). Their chrono-stratigraphic correlation encompasses 15 units and dates to ~450 ka. Roettig et al. (2019) derived a sea-level dependency of the dune archives. They attribute highest sand supply to starting sea-level drops and increased dust deposition during periods of rising sea level. On Lanzarote a stratigraphic description exists only from the Mala dune complex (von Suchodoletz et al., 2013). Von Suchodoletz et al. (2013) discussed middle- to late Pleistocene ages (the dating ranges from ~500 ka to ~50 ka) of the whole Mala dune complex, which encompasses eight so-called palaeosurfaces which are layers that seem related to periods of higher dust supply.

In order to put the sedimentary processes on the Eastern Canary Islands into a context with the well-known late Pleistocene climate development of the northeast Atlantic region, we investigate in this article eolian sediments of Lanzarote to identify possible influences of climatic changes on millennial time scales, such as H Events. The focus of the study is on the multiple dark brown layers rich in dust and iron oxides which initially and for a long time were interpreted as a product of soil formation. This article presents a new interpretation based on new infrared stimulated luminescence (IRSL) age determinations and grain size analyses from a newly sampled Pleistocene dune profile close to the village of Muñique in northern Lanzarote (Fig. 1) and a revision of already published information.

**Figure 1.** (colour online) Locations of Lanzarote and sampling site Muñique and generalized modern wind system of northwest Africa that supplies dust to the Eastern Canary Islands.



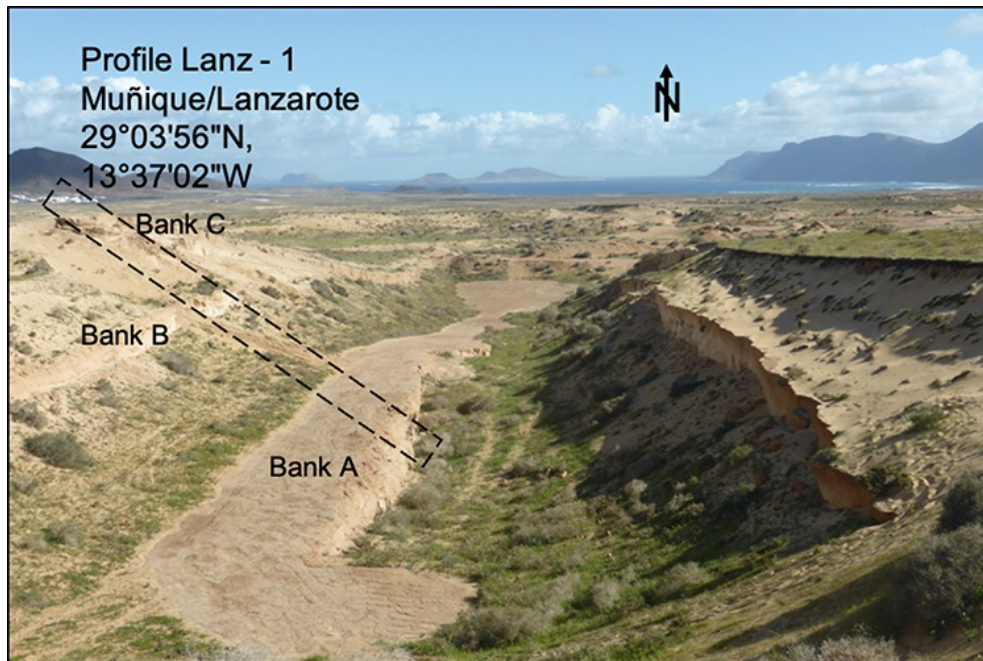
## MATERIAL

The eolian dune deposits on the Eastern Canary Islands mainly consist of generations of a variable mixture of biogenic calcareous marine sediments from the island's shelf area and siliceous eolian dusts from Africa (Muhs et al., 2010; Meco et al., 2011; Faust et al., 2015; Roettig et al., 2017; Roettig et al., 2019). Volcanic eruptions on the island sometimes added ash. The existence of several sequences of the same type gives an indication of recurring climatic conditions (Damnati, 1997; Roettig et al., 2017; Roettig et al., 2019).

In spring 2018, a stacked 10 m profile ("Lanz-1") of eolian deposits was sampled in a sand pit near the village of Muñique on Lanzarote (29°03'56"N, 13°37'02"W) for a new age determination (Figs. 1 and 2). A number of sedimentary sequences can be observed. In general, a sequence consists of three types of deposits (DepoTypes) that are visually different (Ellis and Ellis-Adam,

1993; Edwards and Meco, 2000; Genise et al., 2013). The lower two DepoTypes (DepoTypes 1 and 2) of a sequence consist almost exclusively of light yellowish-brown marine biogenic carbonate silts and sands from the adjacent shelf and small amounts of siliceous dust (10YR, Munsell Colour Chart, 1975). The upper of these two layers (DepoType 2) is characterized by a high proportion of terrestrial gastropods and by calcified brood cells of insects (Ellis and Ellis-Adam, 1993; Edwards and Meco, 2000; Genise et al., 2013). The top DepoType 3 is a strong brown layer (7.5YR, Munsell Colour Chart, 1975) with land snails and brood cells. Its carbonate content is visibly lower than in the DepoTypes 1 and 2, and the dust content is correspondingly higher. In the profile investigated, only one sequence seems to be complete. DepoType 3 forms prominent hard banks in the outcrop, which are marked as Banks A–C in Figure 2.

**Figure 2.** (colour online) Muñique outcrop and position of the stacked profile Lanz-1.



Twenty-four samples were taken from the stacked profile for carbonate content and grain-size analyses. For IRSL dating, three samples were taken from the strong brown layers— samples 6 (BT1707), 13 (BT1708), and 16 (BT1709)—and two samples from the light yellowish-brown parts of the profile— samples 2 (BT1706) and 21 (BT1710).

## METHODS

### Sediment Colours

Colour description was carried out on wet samples with the Munsell Colour Chart (Munsell Color, 1975).

### Determination of carbonate content

The carbonate content of 24 samples was determined with a Scheibler Calcimeter (DIN 18129) after treatment of the air-dried and 2-mm-sieved samples with hydrochloric acid.

### Grain size determination

The measurements of grain size distributions of the 24 samples were performed on bulk sediment with the Horiba LA-950 laser diffraction particle size distribution analyser at the GFZ German Research Centre for Geoscience Potsdam. The air-dried samples were suspended with sodium pyrophosphate for 24 hours. Each sample was measured five times. For this study we used the medians of the fivefold measurements per sample. The values encompass 80 classes ranging from 0.058  $\mu\text{m}$  to 2500  $\mu\text{m}$ .

### Infrared stimulated luminescence (IRSL) dating

Both the detrital carbonate sediments and the land snails embedded in the sediment profile cannot be described with certainty as being autochthonous. For each of the components there is a higher probability that older material has been relocated. Thus, using the  $^{14}\text{C}$  method for dating would not give reliable ages for the deposition of the DepoType 3 type sediments. Therefore, IRSL dating, which documents the time elapsed since the last exposure of the sediment surface to daylight, was chosen to determine their deposition age. The main caveat of IRSL signals from feldspar is that they are reported to fade over time ('anomalous fading') (Wintle, 1973), causing age underestimation. In this study, however, we employed an IRSL protocol for

equivalent dose ( $D_e$ ) estimation for which we could not detect any substantial fading over laboratory time scales.

## Samples and sample preparation

Five sediment samples from profile Lanz-1 were taken for luminescence dating to determine their burial age. Sampling was realized by hammering steel tubes horizontally into the cleaned profile and collecting representative material in the surrounding (<30 cm) of the luminescence sample for assessing the environmental dose rate. In the laboratory, sample material extracted from the center of the steel tube was further processed under subdued red light ( $640 \pm 20$  nm) conditions following routine methods to isolate polymineral grains in the ~4–11  $\mu\text{m}$  range ('fine grains'; see Supplementary Materials for details).

## Dose rate determination

The dose rate was determined on milled (<63  $\mu\text{m}$ ) sediment taken from the surrounding of the IRSL sampling holes using thick-source  $\alpha$ -counting analysis (Aitken, 1985; Zöller and Pernicka, 1989) for the U and Th concentration as well as inductively coupled plasma - optical emission spectrometry (ICP-OES) for the K concentration. The final dose rate was calculated with the DRAC software (v1.2; Durcan et al., 2015) using parameters as specified in the Supplementary Materials.

## Instrumentation and protocols for equivalent dose determination

IRSL was measured with a Risø DA15 TL/OSL reader featuring a DA20 control unit (Bøtter-Jensen et al., 2003). (See Supplementary Materials for further details).

The protocol applied here to determine the  $D_e$  was used in an earlier study on Fuerteventura (Faust et al., 2015) and builds on previous experience by Preusser (2003), von Suchodoletz et al. (2008) and Rother et al. (2010). It is based on a single-aliquot regenerative (SAR) routine (Murray and Wintle, 2006), including a preheat of 270°C for 120 s prior to IRSL readout for 300 s at 90% LED power. A resting period of 20 minutes between the preheat after artificial irradiation and IRSL measurement aims to minimize or even avoid the problem of anomalous fading (Wintle, 1973) of the feldspar component in the polymineral samples (Faust et al., 2015). The protocol with all relevant parameters is shown in Supplementary Table S1.

To test this protocol for its suitability to reproduce known doses with the studied samples, a dose recovery test (DRT) was conducted on sample BT1709. Likewise, fading tests were carried out on the same sample to assess the impact of potential anomalous fading on the  $D_e$  results. Protocol parameters are described in the Supplementary Materials.

Data reduction to obtain  $D_e$  values was done using the Analyst program (v4.31.9; Durcan et al., 2015 [Q4]) and taking the first 2 s of the IRSL decay curve minus a background averaged from the last 50 s to construct dose-response curves. These were obtained by fitting a single saturating exponential function to the data points. All aliquots not meeting the acceptance criteria of a recycling ratio within 10% deviation from unity, a recuperation rate <5%, a test dose error <10%, and a signal larger than three times the background were rejected. A systematic uncertainty of 3% was added to the  $D_e$  value to account for uncertainties in  $\beta$ -source calibration.

## Climate Modelling

In a set of glacial/deglacial simulations by Ziemen et al. (2019), H Events occurred as internal model. Zieman et al. used a periodically synchronous version of the coupled model system consisting of the coarse resolution climate/dynamical vegetation model ECHAM5 (T31L19)/MPIOM(GR30L40)/LPJ (Mikolajewicz et al., 2007) coupled to a northern hemisphere set-up of the ice sheet model mPISM (20 km, Ziemen et al., 2014). Land sea mask and ocean topography were fixed at 21ky state; orography, glacier mask, and river routing were interactively coupled. To derive the pattern of a typical H Event, the composite of five individual H Events was computed (Ziemen et al., 2019).

The composite analysis of wind directions, wind strengths, and precipitation were analysed from a long glacial simulation with a coupled atmosphere–ocean–vegetation–ice sheet model (Ziemen et al., 2019). In this article, we focus on three different atmospheric pressure levels (925 hPa, 775 hPa, and 500 hPa) and on precipitation during three phases of the ice shield surges identified (pre-surge, surge, post-surge) which are representative for the two major wind systems that deliver dust to the Canary Islands: the trade wind system close to the ground and the higher Saharan Air Layer. In this study we use only the summer situation (June, July, and August) because dust mobilization in the Sahel occurs mostly during summerly convective weather events (thunderstorms).

# RESULTS

## Soil Colours

The soil colours according to Munsell (Munsell, 1975) range from a light-yellow brown in the carbonate sands to a dark brown in the clayey dust layers (Table 1).

**Table 1.** Munsell colours of profile Lanz-1. The characters in the first column indicate the sediment DepoTypes 1 (standard red), 2 (standard italics green) and 3 (bold blue) as displayed in Figure 4.

Sample	H Events	HUE	Value/ Chroma	Names
<b>24</b>	HE1?	7.5 YR	4/4	brown to dark brown
<b>23</b>		7.5 YR	4/4	brown to dark brown
<b>22</b>		10 YR	6/4	light yellowish brown
<b>21</b>		10 YR	6/4	light yellowish brown
<b>20</b>		10 YR	6/4	light yellowish brown
<b>19</b>		10 YR	6/4	light yellowish brown
<b>18</b>		10 YR	6/4	light yellowish brown
<b>17</b>	HE2	7.5 YR	4/6	strong brown
<b>16</b>		7.5 YR	4/6	strong brown
<b>15</b>		7.5 YR	4/6	strong brown
<b>14</b>		7.5 YR	5/6	strong brown
<b>13</b>	HE4	7.5 YR	5/6	strong brown
<b>12</b>		7.5 YR	4/6	strong brown
<b>11</b>		7.5 YR	5/6	strong brown
<b>10</b>		10 YR	6/4	light yellowish brown
<b>9</b>		10 YR	6/4	light yellowish brown
<b>8</b>		10 YR	6/4	light yellowish brown
<b>7</b>	HE7a	7.5 YR	4/6	strong brown
<b>6</b>		7.5 YR	4/4	brown to dark brown
<b>5</b>		7.5 YR	4/4	brown to dark brown
<b>4</b>		10 YR	5/4	yellowish brown
<b>3</b>		10 YR	5/3	brown
<b>2</b>		10 YR	5/3	brown
<b>1</b>		10 YR	5/3	brown

### Carbonate content and grain size

The sediment of Lanz-1 consists mainly of marine biogenic calcareous silt and sands and siliceous eolian dust. Carbonate contents are shown in Table 2 and Figure 4.

**Table 2.** CaCO<sub>3</sub> content and accumulated size classes [Q<sub>2</sub>] 0.1–1.0 µm, 1–60 µm and 60–2500 µm (based on Figure 3). The characters in the first column indicate the sediment DepoTypes 1 (standard red), 2 (standard italics green) and 3 (bold blue) as displayed in Figure 4.

Sample No.	H Event	CaCO <sub>3</sub>	0,1 µm - 1,0 µm	1,0 µm - 60,0 µm	60 µm - 2500 µm
		%	%	%	%
24	HE1?	73,4	10,17	21,11	67,70
23		76,5	6,53	19,55	72,09
22		80,3	4,62	3,97	91,07
21		86,3	0,51	0,00	99,41
20		83,3	0,32	1,63	98,12
19		83,1	1,74	0,00	98,16
18		83,7	2,36	0,00	97,82
17	HE2	67,7	10,84	29,84	59,26
16		64,1	10,99	25,00	63,94
15		73,7	11,02	18,67	70,20
14		77,9	6,75	17,04	75,86
13	HE4	76,8	9,77	25,12	65,66
12		78,1	9,10	18,25	71,59
11		82,1	9,44	17,25	72,58
10		86,5	4,28	10,84	84,48
9		90,1	4,86	0,48	94,14
8		88,3	2,04	0,00	97,99
7	HE7a	79,7	24,26	10,96	64,49
6		49,9	12,03	39,70	48,35
5		59,5	18,96	27,51	52,38
4		67,6	13,45	16,34	69,66
3		61,5	1,15	0,00	98,81
2		64,6	2,91	0,12	96,69
1		63,2	0,29	0,16	99,63

The measured 80 size fractions of grain size in the bulk sediment samples can be summarized into three size classes: 0.1 µm–1.0 µm, 1 µm–60 µm, and > 60 µm (Fig. 3). Classes are separated by stretches of concentration close to zero percent. Figure 4 and Table 1 show the grain size distributions of the three classes in all samples. The smallest class (0 µm–1 µm) occurs in all samples and ranges between 0.3 and 11%. The silt class (1µm–60 µm) is largely lacking in the light-coloured parts of the profile. Within this class the highest amounts of up to 40% occur in the dark brown sediment layers. In the coarsest class (60µm–2500 µm), minimum values of about 60% occur in the dark brown layers and close to 100% in the lightest part of the profile. The percentages in the three individual classes clearly depend on the type of sediment. With increasing red colouring, i.e., decreasing CaCO<sub>3</sub> content, the percentages of the two small classes increase and the coarsest class decreases (Fig. 5). In the lowest part of the profile (samples 1–3), the two classes < 60 µm obviously contain a higher proportion of coarse volcanic ash, so that the carbonate content is significantly reduced. Comparing the sizes of the dominant fraction of a sample, i.e., the measured fraction

with the highest amount (%), one observes a coarsening within grain size class 3 from the bottom of the profile towards its top (Fig. 6). Overall, the values in this profile correspond to those usually found in the eolian sediments of Lanzarote and Fuerteventura (von Suchodoletz et al., 2009; Muhs et al., 2010; Faust et al., 2015; Roettig et al., 2017; Roettig et al., 2019).

**Figure 3.** (colour online) Spectra of 80 grain size classes from profile Lanz-1. The size classes can be grouped into three main classes (0.1–1.0  $\mu\text{m}$ , 1–60  $\mu\text{m}$ , and 60–2500  $\mu\text{m}$ ) which are separated by grain size classes close to zero. DepoType 1 red lines, DepoType 2 green lines, DepoType 3 blue lines. Gray lines mark DepoType 1 samples 1–3 containing volcanic ash.

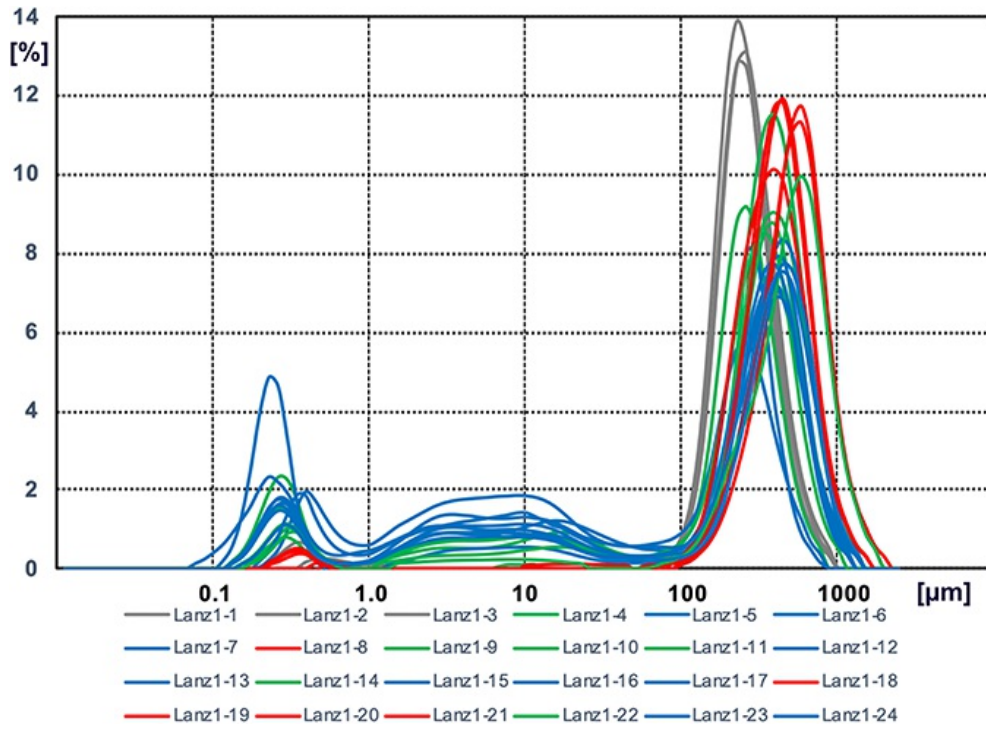


**Figure 4.** (colour online)  $\text{CaCO}_3$  content and Volume-% of the three generalized grain size class 1 (0.1–1.0  $\mu\text{m}$ ), class 2 (1–60  $\mu\text{m}$ ) and class 3 (60–2500  $\mu\text{m}$ ). The data are listed in Table 2. Banks 1–3 refer to Figure 2.

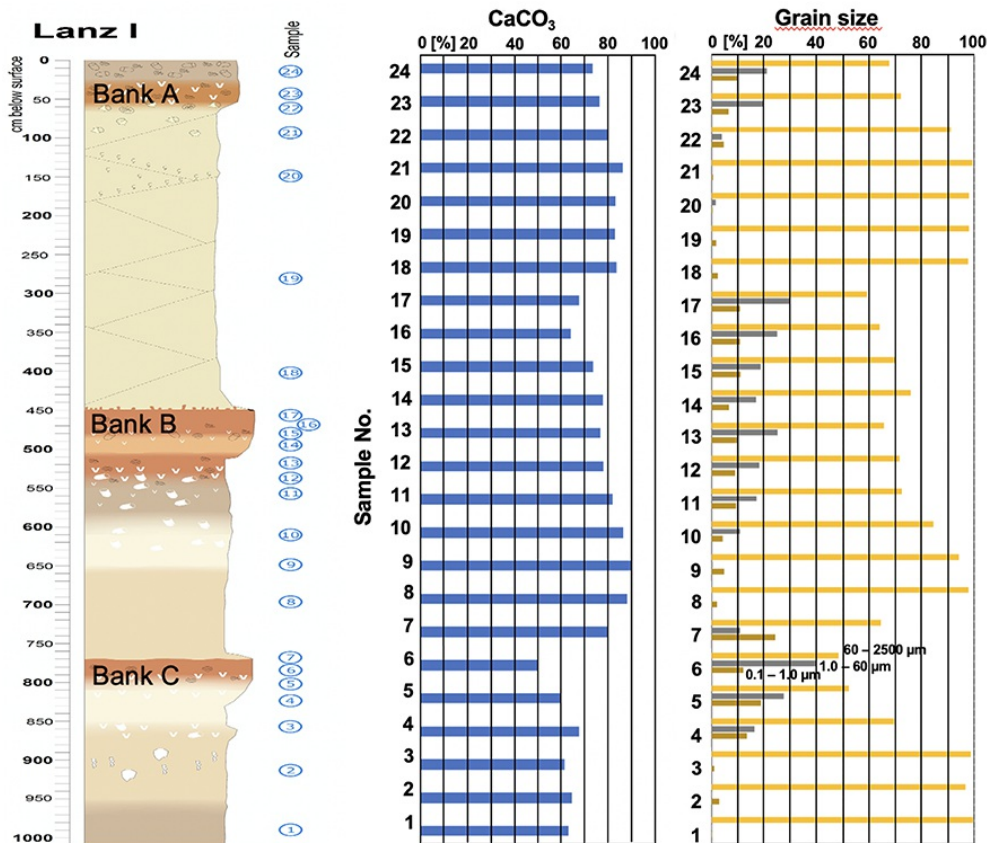


**Figure 5.** Volume-% of grain size classes 0.1–1.0  $\mu\text{m}$  (squares), 1–60  $\mu\text{m}$  (diamonds) and 60–2500  $\mu\text{m}$  (balls) vs.  $\text{CaCO}_3$  content (watch the reverse scale of  $\text{CaCO}_3$ ). Colours mark sediment DepoTypes 1 (red), 2 (green), and 3 (blue). Gray symbols

mark samples with high ash content. Same three numbers sum up to 100%. With increasing volume of the two smaller classes the CaCO<sub>3</sub> content decreases. Consequently, the CaCO<sub>3</sub> content decreases with decreasing volume of the coarsest class. (For interpretation of the references to colour in this figure legend, the reader is referred to the web version of this article.)

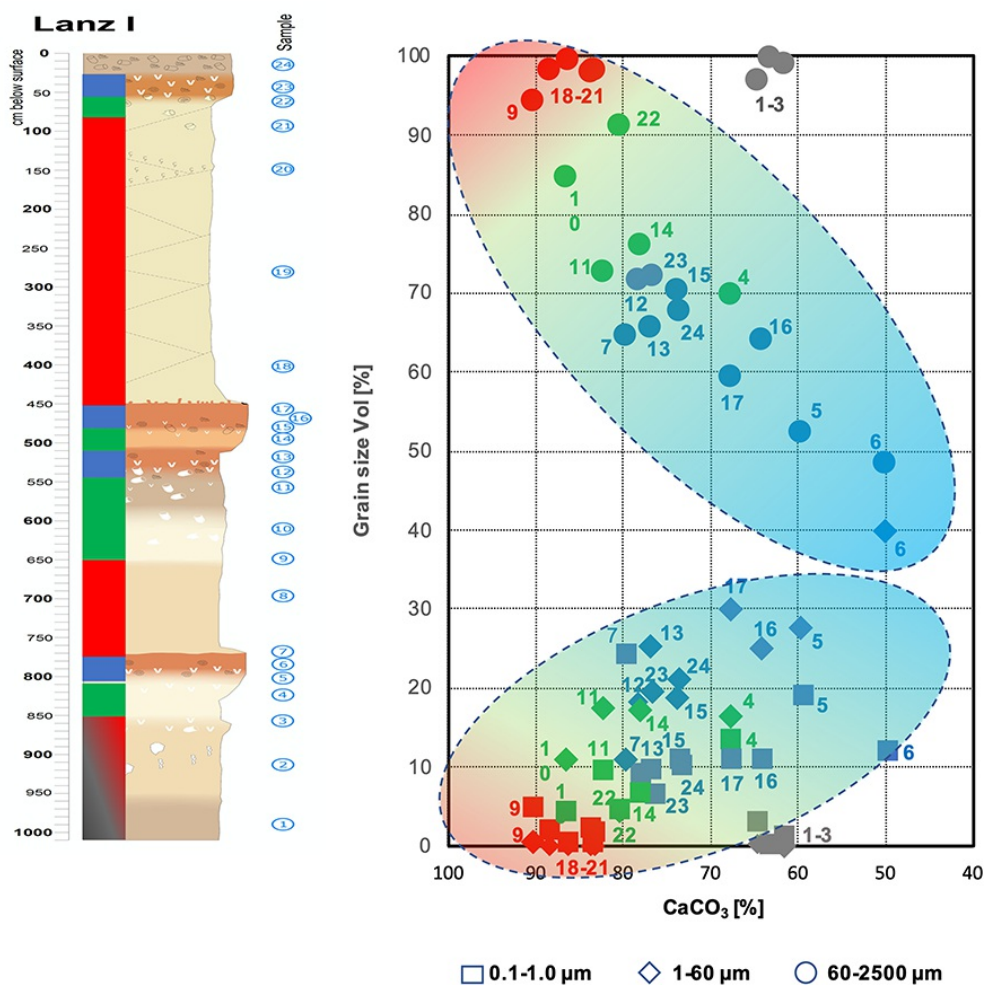
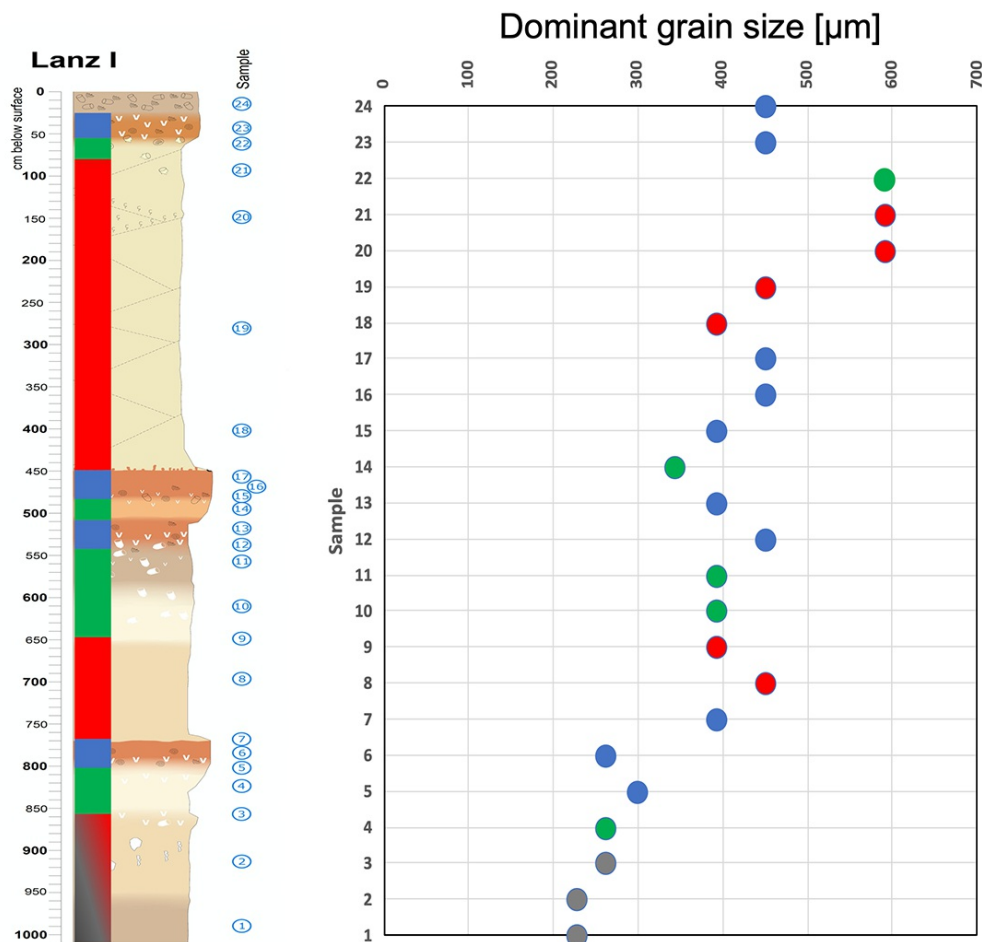


**Figure 6.** (colour online) The dominant grain size class in the profile Lanz-1 increases from the bottom towards the top. However, this does not necessarily mean an increase in wind speed during deposition.



## IRSL dating

The results of the DRT indicate that for sample BT1709 a known dose can be well recovered within 3% deviation for the five aliquots analyzed, and therefore the chosen protocol seems to be appropriate for accurate dose measurements from the sampled sediments at Lanzarote.

The fading test conducted on sample BT1709 indicates that on laboratory time scales there is no detectable IRSL signal loss, or only minor IRSL signal loss, since the fading rates of four out of five analyzed aliquots are  $<1.2\%/decade$  (see Supplementary Figure S2). The averaged  $g$ -value from the five measured aliquots is  $1.2 \pm 0.7\%/decade$ . These low fading rates and the inherent uncertainties related to the fading correction procedures do not justify the application of such routines for the samples under study. Furthermore, fading rates in the order as determined in this investigation are frequently considered as laboratory artefacts (e.g., Thiel et al., 2011). Therefore, we infer that the chosen SAR protocol produces IRSL signals with sufficient stability for accurate dating results.

The application of the aliquot acceptance criteria (see the section on instrumentation and protocols, above) leads to acceptance ratios between 36% (BT1706) and 100% (BT1707 and BT1709). Sample BT1710 is an exception, for which about 2/3 of all analyzed aliquots passed the recycling ratio test, but none of them passed the recuperation test with recuperation ratios consistently  $>6.5\%$ . Therefore, the resulting age has to be treated with caution, and the age inversion in relation to underlying samples might be caused by the poor performance of the SAR protocol for this sample. Overdispersion values for all samples range between 0% and 12%, the latter value being surprising for fine grain separates where averaging effects are supposed to lead to narrow dose distributions (Duller, 2008). However, since the reason for this comparatively large spread in  $D_e$  values remains unclear and cannot be unequivocally attributed to different degrees of bleaching of individual grains, no age model was applied. Instead, the  $D_e$  value used for age calculation was obtained by calculating the unweighted average of all accepted aliquots. These dose values vary between  $27.7 \pm 1.3$  Gy (BT1710) and  $88.0 \pm 3.1$  Gy (BT1707). A representative  $D_e$  distribution is shown as an abanico plot (Dietze et al., 2016) in Supplementary Figure S1b, together with exemplary IRSL decay and dose response curves.

Environmental dose rates are comparatively low with values between  $0.83$  and  $1.53$  Gy  $\text{ka}^{-1}$ , owing to the high content of primary carbonates in the sediments. Resulting ages are listed in Table 3. Lanz-1 profile starts with  $58.8 \pm 4.6$  ka for the lowermost sample BT1706 taken from the lowest part of the profile. Considering  $1\sigma$  uncertainty levels, this age is younger than that obtained for the overlying sample BT1707 ( $71.6 \pm 4.6$  ka; though statistically indistinguishable within  $2\sigma$ ) which derives from a laterite-like layer

rich in dust. The following two samples BT1708 and BT1709 are in stratigraphic order and document that the two layers of dark brown sediments accumulated around 36 ka and 24 ka, respectively. The uppermost sample BT1710 showed IRSL characteristics (see above) rendering the obtained age of  $33.3 \pm 2.4$  ka probably unreliable, which might be the cause for the observed age inversion in the upper part of the Lanz-1 section.

**Table 3.** IRSL ages from profile Lanz-1 and the ages of the respective Heinrich Events.

Lanz-1	Lab	Lanz-1	H Events
Sample	Code	Age [ka]	Age [ka]
16	BT1709	$23.6 \pm 1.5$	H2 22 - 24
13	BT1708	$36.3 \pm 2.3$	H4 35 - 38
6	BT1707	$71.6 \pm 4.6$	H7a 72

### Wind directions and wind speed

In Ziemen et al. (2019), long glacial simulations with the coupled ice sheet–climate–vegetation model mPISM/ECHAM5/MPI-OM/LPJ showed recurring ice-sheet collapses (referred to as H Events in the following text). To describe the typical behaviour of these events, Ziemen et al. performed a composite analysis of several events. Three typical phases of a surge event were identified. The pre-surge phase (maximum ice volume, pre-H Event), the surge phase (maximum ice discharge in the Hudson Strait, H Event), and the post-surge phase (minimal ice-sheet volume in northeastern Canada, post-H Event). Since for all three phases and all events 200-year long time slices were selected and for each of the phases a climatology was computed, the sequences of these climatologies thus represents the climatic behaviour of a typical event in the model.

During the H Events, the model showed a weakening of the AMOC by 3.5 Sv, a general cooling of the northern hemisphere with maximal amplitude in the northern North Atlantic and Europe, a southward shift of the Intertropical Convergence Zone (ITCZ) over the Atlantic, and drier conditions over the Sahel. The atmospheric circulation before, during and after the H Events is shown in three different altitude levels: 925 hPa, 775 hPa, 500 hPa (Fig. 7). The left column shows the metric altitudes of these air pressure levels and the resulting wind vectors before an H Event (Fig. 7a<sub>1</sub>–a<sub>3</sub>). The middle (Fig. 7b<sub>1</sub>–b<sub>3</sub>) and the right column (Fig. 7c<sub>1</sub>–c<sub>3</sub>) show the anomalies in the altitude of the respective air pressure, wind vector against the pre-H Event. Although the differences of H Event and post-H Event relative to the pre-H Event situation are rather small, there are visible signals in both upper layers (Fig. 7b<sub>2</sub>, c<sub>2</sub>, and c<sub>3</sub>) that enhance the likelihood for dust transport events from the subtropical-tropical Sahel towards the Canary Islands to occur. The reason for the weak signals might be that the atmospheric model was not tuned to dust transport. The modelled precipitation during these three stages shows this area of the Sahel zone before an H Event being humid, and during and after an H Event being drier (Fig. 8). The latter reveals this region as a potential source of dust rich in kaolinite and iron oxides.

**Figure 7.** (colour online) Geopotential heights and wind vectors in three different altitudes of the three ice shield surging phases (H Events) during summer (JJA). Columns a<sub>1</sub>–a<sub>3</sub> show the geopotential height of three different atmospheric pressure levels and wind vectors. Columns b<sub>1</sub>–b<sub>3</sub> and c<sub>1</sub>–c<sub>3</sub> show the anomalies of all parameters relative to the “pre-H Event” situations during “H Event” and “post-H Event”.

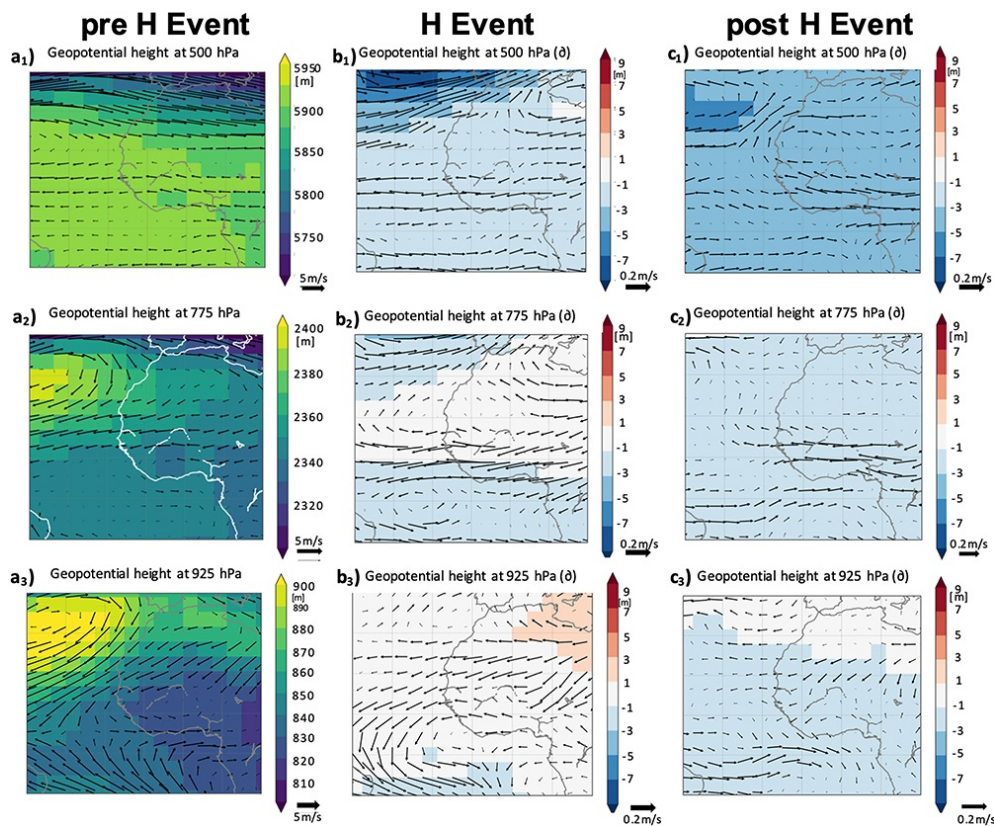
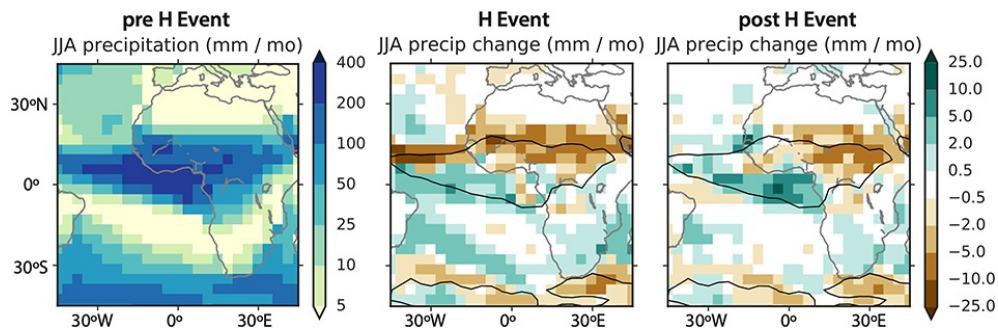


**Figure 8.** (colour online) Summer season (JJA) precipitation before the H Event, and JJA precipitation changes during and after the H Event. In the change plots, the black outline marks 100 mm/month precipitation before the event.



## DISCUSSION

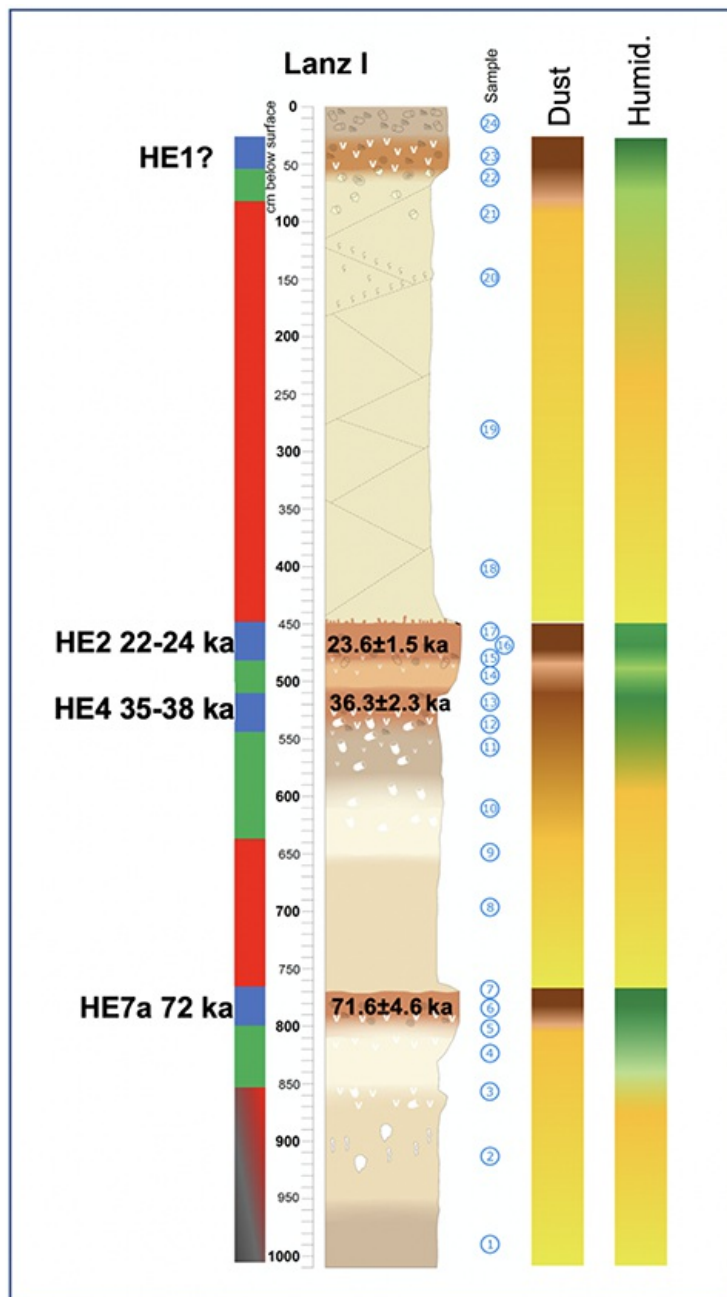
Basically, the Pleistocene dune sediments of Lanzarote (and Fuerteventura) consist of multiple sequences with a three-stage structure (DepoTypes 1–3). DepoType 1 forms the base of a sequence with the highest content of  $\text{CaCO}_3$  and the lowest dust content. Although there are (uncalcified) brood cells, no other hints of vegetation exist in this DepoType. The lack of traces of vegetation and of dust from the African continent points obviously to rather dry conditions. Unfortunately, the dating in this sediment type with IRSL, as well as with the aminostratigraphical method (Ortiz et al., 2006), is very problematic, so that no statement can be made about the time or timing of their deposition. In DepoType 2, the granulometric composition of the coarse detrital sediment (i.e., biogenic carbonate sands) remains about the same as in DepoType 1 (Figs. 3–6). The onset of DepoType 2 is indicated by the abrupt appearance of land snails and calcified brood cells, the increase of the dust class (0.1–1  $\mu\text{m}$ ) and the appearance of the class with 1–60  $\mu\text{m}$ . In DepoType 2 sediments on Lanzarote and Fuerteventura, the dust fraction consists mainly of illites, with a small amount of kaolinite (5–10%) and iron (Roettig et al., 2017). Possibly, a sparse shrub vegetation similar to the present vegetation formed the habitat of the land snails. This type of vegetation presently exists with an average annual precipitation of 116 mm/a and 19 days with rainfall >1 mm (Spanish State Meteorological Agency; Menéndez et al., 2014). Thus, both the gastropod fauna, the lithified brood cells, and the appearance of siliceous dust indicate an increase towards some but still very low precipitation, possibly through changes in the wind system. Since no other calcification than lithified brood cells can be observed in DepoType 2, calciferous pore water flow occurred only over extremely short distances, so that solution and precipitation happened at virtually the same place (see Roettig et al., 2019).

The brown clayey DepoType 3 deposits on Lanzarote and Fuerteventura are characterized on average by high contents of iron, quartz, and kaolinite (15–20%). This is much higher than in DepoTypes 1 and 2 (Menéndez et al., 2007; Muhs et al., 2010; Menéndez et al., 2014; Roettig et al., 2017). Muhs et al. (2010) and Roettig and Faust (2018) exclude the occurrence of kaolinite on

Lanzarote being from soil formation and assumed a higher dust supply from adjacent Africa. A stronger post-depositional soil formation has been unlikely under the relatively dry atmospheric conditions prevailing during the last glacial period in the northeast Atlantic region and in northwest Africa (Mulitza et al., 2008; Tjallingii et al., 2008). As in DepoType 2, this is also supported by the general lack of concurrently pedogenic decalcification and CaCO<sub>3</sub> enrichment.

Although the grain size measurements were carried out on the total sediment, conclusions on the input of silicate dust can be drawn from the changes in CaCO<sub>3</sub> content and grain size classes since no other material exists in the samples. In particular, the size classes 0.1–1 µm and 1–60 µm are likely to be of completely allochthonous origin, as they do not occur in the profile sections with the highest CaCO<sub>3</sub> contents (Figs. 4 and 5). A number of grain size analyses were carried out on marine sediment cores near the Canary Islands (Koopmann, 1981; Grousset et al., 1998; Holz et al., 2004; McGee et al., 2013; Skonieczny et al., 2019). Grain sizes of dust range mostly from 2 to 60 µm. Holz et al. (2004) distinguished three endmembers: 2–20 µm (EM3), 5–60 µm (EM2), and 20–60 µm (EM1). These can be traced to some extent in the particle size spectra of the Lanzarote profile (Fig. 3) (Fig. 9). EM1 obviously does not exist as a separate class in the Lanzarote profile. In the profile sections with a high proportion of class 1–60 µm, a bimodality can be observed, with a peak at approx. 2–3 µm and a peak at 10–20 µm. The size class 1–60 µm can therefore be clearly assigned to a wind transport from Africa, analogous to the marine observations. The particle size class 0.1–1 µm was not detected in marine sediments, but this is possibly due to a lack of appropriate measurement technology. We assume that this class is mainly formed by allochthonous kaolinite dust. Authigenous kaolinite is preferably found in this grain size class (Zou and Boley, 2019). In the Lanz-1 profile, there is a relatively clear assignment of the dust supply to the stratigraphic units. In DepoType 1 deposits, there are only small fractions of the class 0.1–1 µm. With the insertion of DepoType 2, the class 0.1–1 µm increases steadily and the class 1–60 µm becomes visible. Both classes then culminate in DepoType 3, and the change from DepoType 3 to the overlying DepoType 1 is abrupt. However, the increase in dust as well as the rise of the dominant grain size fraction towards the top of the profile cannot necessarily be attributed to an increase in wind speed. The corresponding increase in kaolinite and iron is more indicative of changes in the source area and in the atmosphere.

**Figure 9.** IRSL ages and their relation to H Events. The two vertical colour bars propose a sedimentary (dust: brown high content) and climatological (humidity: green higher humidity) evolution of the profile Lanz-1. The colour bar on the left marks DepoType 1 (red), DepoType 2 (green) and DepoType 3 (blue). H Events 3 to 6 are not detectable at this site. The graph exhibits a saw-toothed sedimentary and climatological evolution rather than a sinoidal evolution. (For interpretation of the references to colour in this figure legend, the reader is referred to the web version of this article.)



Roettig et al. (2019) designated these dark brown layers of DepoType 3 as paleosurfaces which were formed during periods of rising sea level with reduced or even stopped carbonate sand deposition. In accordance to Moreno et al. (2001), they attribute best conditions for dust imprint and weak soil formation to terminations of glacials. Moreno et al. (2001) identified the influence of the Earth's orbital parameters on the dust supply to the Canary Islands region. However, the new IRSL ages in profile Lanz-1 attach the formation of DepoType 3-type layers to H Events (Table 3). The ages in these layers are clearly consistent with the ages of the H Events HE2, HE4 and HE7a in northeast Atlantic marine deposits and elsewhere (Table 3 and Fig. 9). An age from a nearby, still unprocessed profile Lanz-2 reveals  $21.4 \pm 1.4$  ka that is in good agreement with HE2. There are more publications with age dating of massive dust layers, but these have not been assigned to H Events. For example, at Melián (Fuerteventura), the lower and upper limits of a dust layer were dated  $16.6 \pm 1.2$  ka and  $14.9 \pm 1.2$  ka, which encloses quite exactly to the period of HE1 (Roettig et al., 2019). Aminostratigraphic age determinations carried out on snails in dune sediments of the eastern Canary Islands have revealed similar ages (Ortiz et al., 2006). Although these ages are under discussion (Meco et al., 2011), some of the dust layers have approximately the same ages as the H Events 1 to 4, but with relatively large uncertainty ranges. However, an assignment to H Events did not take place. Neither study reveals any signs of higher-frequent climatic information, such as Dansgaard-Oeschger events, although the latter occur in marine sediments on northwest Africa and the African continental margin (Carlson and Prospero, 1972; Prospero and Mayol-Bracero, 2013; Jaramillo-Vélez et al., 2016; Weinzierl et al., 2017). Interestingly, although the amino ages of Ortiz et al. (2006) were determined on snails, the ages between the dust horizons are mostly younger than the ages retrieved from the dust layers above, comparable to the IRSL ages. One possible explanation could be that DepoTypes 1 and 2 contain much older, relocated material.

The wind regime in the Canary Islands is determined by the trade wind that blows close to the surface from north-east and by the

Saharan Air Layer which results in easterly winds (Fig. 1; Carlson and Prospero, 1972; Prospero and Mayol-Bracero, 2013; Jaramillo-Vélez et al., 2016; Weinzierl et al., 2017). The Calima is a component of the Saharan Air Layer. In the summer it mainly brings dry, hot air and silty dust (Carlson and Prospero, 1972; Prospero and Mayol-Bracero, 2013; Jaramillo-Vélez et al., 2016; Weinzierl et al., 2017). The source areas of the dust can be identified by its mineral composition; dust from the Sahara is dominated by illite, dust from the Sahel by kaolinite (Stager et al., 2011; Bouimetarhan et al., 2012). The particle size distributions of the dust depend essentially on the particle size, the length of the transport path, and the wind force (Stager et al., 2011; Bouimetarhan et al., 2012).

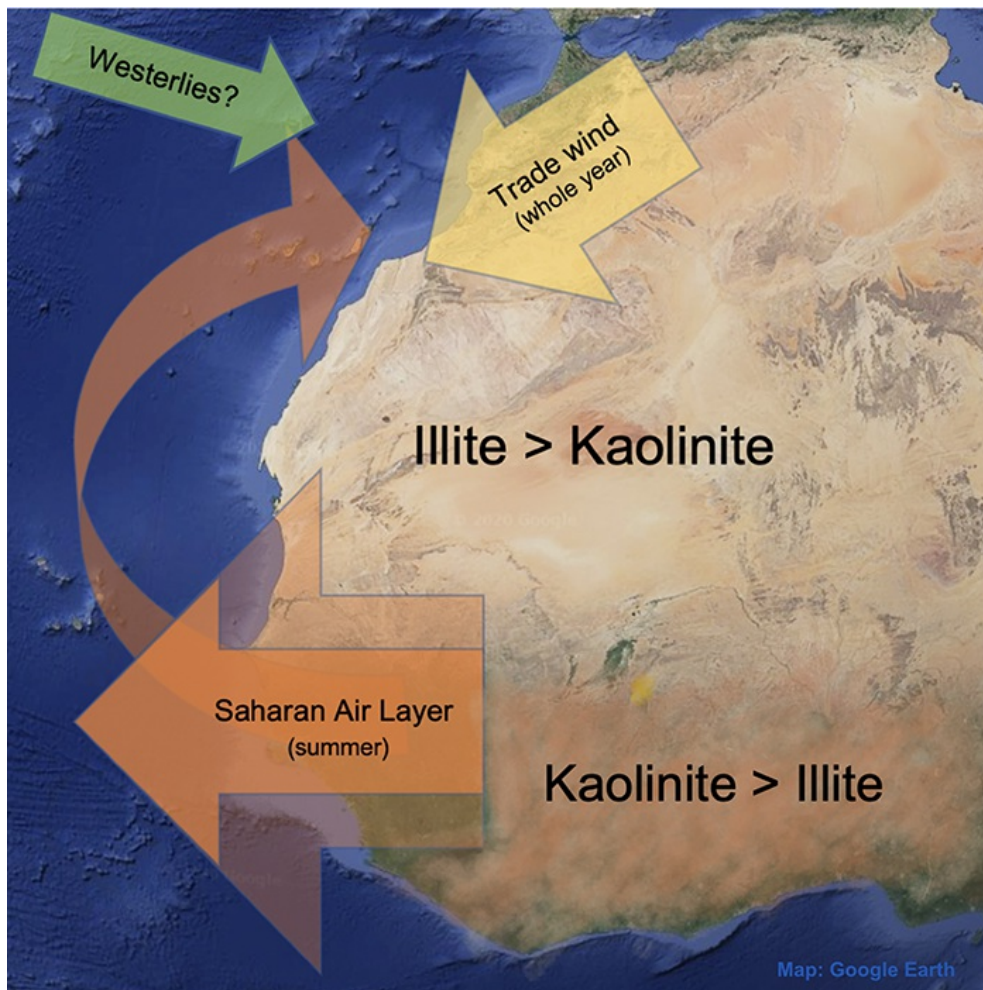
During the last glacial maximum (LGM), the transport of dust is estimated to have been up to 90% greater than it is today (Stager et al., 2011; Bouimetarhan et al., 2012). For the area of the Canary Islands, Stager et al. and Bouimetarhan et al. modelled a dust deposition of about 10 g/m<sup>2</sup>/year. McGee et al. (2013), Williams et al. (2016) and Skonieczny et al. (2019) estimated the dust during LGM to be two to four times higher than today. Stager et al. (2011) and Bouimetarhan et al. (2012) identified no difference in the spatial structure of dust transport during the LGM. However, it is important to mention that the LGM is not equivalent to a H Event. Especially during H Events 1 and 2, the climate in the northern hemisphere was more extreme than during the LGM (McGee et al., 2013; Williams et al., 2016; Skonieczny et al., 2019). Consequently, the climatic conditions of the LGM cannot easily be compared with those of a H Event.

McGee et al. (2013), Williams et al. (2016), and Skonieczny et al. (2019) presumed dust transport from the Sahel to the Canary Islands within a glaciation through a high-pressure cell above the Sahara which formed during winter times. However, in the Sahel zone dust is mobilized during summer by convective weather events (thunderstorms) that lift dust to greater heights; the dust is then transported across the Atlantic Ocean (von Suchodoletz et al., 2008, 2010). The enhanced dust mobilization and deposition during H Events is supported by elevated dust deposition on the marine northwest African continental margin (McGee et al., 2013; Williams et al., 2016; Skonieczny et al., 2019) and in the Mid-Atlantic Ocean (Middleton et al., 2018). Von Suchodoletz et al. (2008 and 2010) have identified a link between dust supply from the Sahel and the climatic variability in northeast Atlantic region during glaciations. Roettig et al. (2019) interpreted the elevated contents of iron, quartz, illite, and especially kaolinite in the DepoType 3 deposits as an increased dust supply from the Sahara. The content of kaolinite and iron in African soils increases from the Sahara towards the subtropical-tropical Sahel (Ojanuga, 1979; Caquineau et al., 1998; Muhs et al., 2010; Scheuven et al., 2013; Formenti et al., 2014; Ravelo-Pérez et al., 2016). Thus, while at present the Saharan dust is generally richer in mica than in kaolinite (McManus et al., 1999; Bard et al., 2000; de Abreu et al., 2003; Naughton et al., 2009; Voelker et al., 2009; Rodrigues et al., 2017), there must have been a modification in the source area of the dust during H Events. Therefore, it seems plausible that beginning with DepoType 2, the subtropical/tropical Sahel zone with its latosols is a dust source area of growing importance, reaching maximum importance during H Events. The onset of a vegetational cover in DepoType 2 and into DepoType 3 could be a joint effect of increasing precipitation and an increasing supply of dust, which included fertilizing iron and phosphate (McManus et al., 1999; Bard et al., 2000; de Abreu et al., 2003; Naughton et al., 2009; Voelker et al., 2009; Rodrigues et al., 2017). To what extent sediment from the African continental shelf contributed to the dust deposition on the Canary Islands during low sea levels can be determined neither from the literature nor from our own investigations. Air-borne and river-borne sediments from the Sahel were deposited on the shelf and there is a similarity in the grain size distribution in the <100 µm fraction of dust on the Canary Islands (this study) and in marine deposits (McManus et al., 1999; Bard et al., 2000; de Abreu et al., 2003; Naughton et al., 2009; Voelker et al., 2009; Rodrigues et al., 2017). However, the African shelf is dominated by silicate sediment, making it less of a source of dust for the Canary Islands, especially in DepoTypes 1 and 2 (Jullien et al., 2007; Deplazes et al., 2013; Handiani et al., 2013; Blazey et al., 2014).

The oceanic archives indicate colder climatic conditions in the northeastern Atlantic Ocean during the last glacial than are present today (McManus et al., 1999; Bard et al., 2000; de Abreu et al., 2003; Naughton et al., 2009; Voelker et al., 2009; Rodrigues et al., 2017). Based on the available information, a basic picture of the development of dune sedimentation during abruptly changing Pleistocene climatic conditions on Lanzarote can now be constructed (Fig. 10). The cold atmospheric conditions above the very cold North Atlantic Ocean shifted during these periods down to the southern limit of the Sahara, creating stadial climatic conditions (Collins et al., 2013). During the H Events, the tropical rain belt (ITCZ) was more southern than it is today (Jullien et al., 2007; Deplazes et al., 2013; Handiani et al., 2013; Blazey et al., 2014). The increase in the grain size class 1–60 µm in DepoTypes 2 and 3 in profile Lanz-1 could be an indicator of an increasing storminess (Bozzano et al., 2002; Bouimetarhan et al., 2012). A more southerly track of the Westerlies could be responsible for the slightly more humid conditions during DepoTypes 2 and 3, too (Naughton et al., 2009). However, the annual precipitation arriving on Lanzarote probably has been rather low. The polar jet stream, which marks the boundary between the polar and the subtropical atmosphere, reached its most southerly position during the H Events (Naughton et al., 2009; Ziemann et al., 2019). According to Ziemann et al. (2019), during and after H Events wind vectors at the 775 hPa and 500 hPa levels representative for the Saharan Air Layer (SAL) allowed dust transport from the subtropical-tropical Sahel zone towards the Canary Islands only in summer. Although the change in the wind vectors at the 775 hPa and 500 hPa levels (relative to the pre-H Event situation) during and past a H Event is not particularly pronounced (Figs. 7b<sub>1</sub>, b<sub>2</sub>, c<sub>1</sub>, c<sub>2</sub>), there is a high probability of this transportation route as can be inferred from the general mineralogical and chemical

composition of the DepoType 3-type deposits on the Canary Islands. Thus, according to the model results of Ziemeň et al. (2019), it seems evident that during H Events the atmospheric dynamics with respect to dust mobilization by summer thunderstorms were quite similar to the present-day observations of Gasse (2000), Mulitza et al. (2008), Tjallingii et al. (2008), Itambi et al. (2009), Naughton et al. (2009), and Bouimetarhan et al. (2012), but with a more southerly source area of dust than today. In addition, due to the modelled dryer conditions during and perhaps directly after a surge event (Fig. 8), together with stronger trade winds and an intensified African Easterly Jet (AEJ), the Sahel had been a much larger source of dust than during the humid periods prior to H Events (Gasse, 2000; Mulitza et al., 2008; Tjallingii et al. 2008; Itambi et al., 2009; Naughton et al., 2009; Bouimetarhan et al., 2012). A generalized scheme of the wind situation and the mineralogy of the source areas is given in Figure 10. Subsequent to a H Event, when the AMOC resumed and the North Atlantic Ocean became warmer, the atmospheric system moved back to its most northerly interstadial position. This was obviously a phase of stronger trade winds and the driest climatic conditions on the Canary Islands responsible for the formation of DepoType 1, as can also be seen on the Iberian Peninsula (Naughton et al., 2009).

**Figure 10.** (colour online) Generalized wind system supplying dust to Lanzarote during H Events and mineralogical composition of the source areas (compare with Figure 1).



## CONCLUSION

With the help of new age determinations, grain size analyses from the Lanz-1 profile, atmospheric data extracted from a published model study, and support provided by data from earlier works on the Pleistocene dune sediments, a new interpretation of the dunes' depositional conditions can be justified. The genesis of the dark brown, highly dusty sediment layers (DepoType 3 in this paper) does not appear to be the result of autochthonous soil or surface formation (Criado et al., 2012; Roettig et al., 2019). The sediment layers are now interpreted as the consequence of changes in atmospheric conditions over northwest Africa and the North Atlantic during H Events that led to a strong dust transport rich in kaolinite and iron compounds from the Sahel towards the Eastern Canary Islands.

The strongly changing climatic conditions on millennial time scales during the glaciations obviously had a major influence on the eolian sedimentary conditions and the source areas of the dust delivered to the Canary Islands. The alternation of Heinrich stadials and interstadials, which originated from repetitive collapses of the North Atlantic ice sheets producing very cold North Atlantic surface water and the successive resumption of the AMOC with its temperate surface water led obviously to a three-stage sequential depositional history of eolian sediments on the Canary Islands. Recent dating of Pleistocene eolian sediments from an

outcrop near Muñique/Lanzarote clearly shows that in a depositional sequence the dust content in the DepoType 3-type deposits mainly originated from elevated supplies from the subtropical/tropical Sahel zone during H Events rather than from soil formation. From the results of the particle size analysis it can be concluded that, with the start of DepoType 2, dust was increasingly transported from the Sahel towards the Canary Islands. The peak was reached in DepoType 3. Wind data extracted from a modelling study on the behaviour of the polar jet before, during and after a H Event provide supporting evidence for a modified atmospheric system that allows dust transport during and after ice sheet collapses from the Sahel towards the Canary Islands. Except for DepoType 3, the internal timing of the eolian sequences is difficult or even impossible to achieve when using IRSL dating because of the lack of sufficient dust in DepoTypes 1 and 2 for dating. Thus, based on the IRSL ages collected on Lanzarote it remains unclear to which particular climatic states DepoTypes 1 and 2 can be attributed. DepoType 1 seems to be the driest phase, since neither gastropods nor calcified brood cells occur. Assuming a climatic development similar to the western Iberian Peninsula, the climatic conditions at Lanzarote's DepoType 1 could be attributed to the northward retreat of the polar jet after a H event. In DepoType 2 the occurrence of terrestrial gastropods, similar to those living today on a sparse shrub vegetation, indicates slightly increased precipitation as a consequence of an increasing cooling of the North Atlantic prior to a H Event and a successive southward migration of the polar jet. The peak of the southern shift of climate zones that enables Latosol dust transport from the southern Sahel to the Canary Islands is in DepoTypes 3 during H Events. The absence of H Events between 36 ka and 71 ka, either due to erosion or non-deposition, cannot be explained from the Lanz-1 profile.

## SUPPLEMENTARY MATERIAL

The supplementary material for this article can be found at <https://doi.org/10.1017/qua.2020.100>

## ACKNOWLEDGMENTS

The fieldwork was supported by Julia Schlösser and Luisa Zenker (Technische Universität Dresden). The grain size analyses were carried out by Michael Dietze and Carolin Zorn (GeoForschungsZentrum Potsdam). We thank Dominik Faust (Technische Universität Dresden), Inmaculata Menéndez González and Laura Cabrera Vega (Universidad de Las Palmas de Gran Canaria) for fruitful discussions.

This work was financially supported by the German Research Foundation (FA 239/23-1; TU Dresden) and by the German Federal Ministry of Education and Research (BMBF) as a Research for Sustainability initiative (FONA) through the project PalMod (FKZ: 01LP1502A; MPI Hamburg).

## REFERENCES

Munsell soil color charts. 1975. Munsell Color, Baltimore.

**Aitken, M.J.**, 1985. Thermoluminescence dating. Academic Press, Orlando, Florida. [Q3]

**Andrews, J.T.**, 2000. Icebergs and iceberg rafted detritus (IRD) in the North Atlantic: facts and assumptions. *Oceanography*, **13**, 100–108.

**Bard, E., Rostek, F., Turon, J.L., Gendreau, S.**, 2000. Hydrological impact of Heinrich events in the subtropical Northeast Atlantic. *Science* **289**, 1321–1324.

**Blazey, B., Paul, A., Liu, H., Prange, M.**, 2014. Simulation of the intertropical convergence zone displacement and impacts during the Eemian and Heinrich events. In: *EGU General Assembly Conference, Geophysical Research Abstracts* 16, EGU2014-12366-1.

**Bøtter-Jensen, L., Andersen, C.E., Duller, G.A.T., Murray, A.S.**, 2003. Developments in radiation, stimulation and observation facilities in luminescence measurements. *Radiation Measurements* **37**, 535–541.

**Bouab, N., Lamothe, M.**, 1995. Geochronological framework for the Quaternary paleoclimatic record of the Rosa Negra section. (Fuerteventura Canary Islands, Spain). In: Meco, J., Petit-Maire, N. (Eds.) *Climate of the Past*. International Union of Geological Sciences, Unesco, Earth Processes in Global Change. pp 37–42, Las Palmas de Gran Canaria; Universidad, 1997

**Bouimetarhan, I., Prange, M., Schefuß, E., Dupont, L., Lippold, J., Mulitza, S., Zonneveld, K.**, 2012. Sahel megadrought during Heinrich Stadial 1: evidence for a three-phase evolution of the low- and mid-level West African wind system. *Quaternary Science Reviews* **58**, 66–76.

**Bozzano, G., Kuhlmann, H., Alonso, B.**, 2002. Storminess control over African dust input to the Moroccan Atlantic margin (NW Africa) at the time of maxima boreal summer insolation: a record of the last 220 kyr. *Palaeogeography, Palaeoclimatology, Palaeoecology* **183**, 155–168.

**Caquineau, S., Gaudichet, A., Gomes, L., Magonthier, M.C., Chatenet, B.**, 1998. Saharan dust: clay ratio as a relevant tracer to assess the origin of soil-derived aerosols. *Geophysical Research Letters* **25**, 983–986.

- Carlson, T.N., Prospero, J.M.**, 1972. The large-scale movement of saharan air outbreaks over the northern equatorial Atlantic. *Journal of Applied Meteorology* **11**, 283–297.
- Chapman, M.R., Shackleton, N.J.**, 1998. Millennial-scale fluctuations in North Atlantic heat flux during the last 150 000 years. *Earth and Planetary Science Letters* **159**, 57–70.
- Collins, J.A., Govin, A., Mulitza, S., Heslop, D., Zabel, M., Hartmann, J., Röhl, U., Wefer, G.**, 2013. Abrupt shifts of the Sahara-Sahel boundary during Heinrich stadials. *Climate of the Past* **9**, 1181–1191.
- Criado, C., Torres, J.M., Hansen, A., Lillo, P., Naranjo, A.**, 2012. Intercalaciones de polvo sahariano en paleodunas bioclásticas de Fuerteventura (Islas Canarias). *Cuaternario y Geomorfología* **26**, 73–88.
- Damnati, B.**, 1997. Mineralogical and sedimentological characterization of Quaternary eolian formations and paleosols in Fuerteventura and Lanzarote (Canary Islands, Spain). In: *Climates of the Past: Proceedings of the CLIP meeting held June 2–7 1995, Lanzarote and Fuerteventura (Canary Islands, Spain)*, pp. 71–77.
- de Abreu, L., Shackleton, N.J., Schönfeld, J., Hall M., Chapman, M.**, 2003. Millennial-scale oceanic climate variability off the Western Iberian margin during the last two glacial periods. *Marine Geology* **196**, 1–20.
- Deplazes, G., Lückge, A., Peterson, L.C., Timmermann, A., Hamann, Y., Hughen, K.A., Röhl, U., Laj, C., Cane, M.A., Sigman, D.M., et al.**, 2013. Links between tropical rainfall and North Atlantic climate during the last glacial period. *Nature Geoscience* **6**, 213–217.
- Dietze, M., Kreutzer, S., Burow, C., Fuchs, M.C., Fischer, M., Schmidt, C.**, 2016. The abanico plot: visualising chronometric data with individual standard errors. *Quaternary Geochronology* **31**, 12–18.
- Duller, G.A.T.**, 2008. Single-grain optical dating of Quaternary sediments: why aliquot size matters in luminescence dating. *Boreas* **37**, 589–612.
- Durcan, J.A., King, G.E., Duller, G.A.T.**, 2015. DRAC: dose rate and age calculator for trapped charge dating. *Quaternary Geochronology* **28**, 54–61.
- Edwards, N., Meco, J.**, 2000. Morphology and palaeoenvironment of brood cells of Quaternary ground-nesting solitary bees (Hymenoptera, Apidae) from Fuerteventura, Canary Islands, Spain. *Proceedings of the Geologists' Association* **111**, 173–183.
- Ellis, W.N., Ellis-Adam, A.C.**, 1993. Fossil brood cells of solitary bees on Fuerteventura and Lanzarote, Canary Islands (Hymenoptera: Apoidea). *Entomologische Berichten* **53**, 161–173.
- Faust, D., Yanes, Y., Willkommen, T., Roettig, C.B., Richter, D., Suchodoletz, H. von, Zöller, L.**, 2015. A contribution to the understanding of late Pleistocene dune sand-paleosol-sequences in Fuerteventura (Canary Islands). *Geomorphology* **246**, 290–304.
- Formenti, P., Caquineau, S., Desboeufs, K., Klaver, A., Chevaillier, S., Journet, E., Rajot, J.L.**, 2014. Mapping the physico-chemical properties of mineral dust in western Africa: mineralogical composition. *Atmospheric Chemistry and Physics* **14**, 10663–10686.
- Gasse, F.**, 2000. Hydrological changes in the African tropics since the last glacial maximum. *Quaternary Science Reviews* **19**, 189–211.
- Genise, J.F., Alonso-Zarza, A.M., Verde, M., Meléndez, A.**, 2013. Insect trace fossils in aeolian deposits and calcretes from the Canary Islands: their ichnotaxonomy, producers, and palaeoenvironmental significance. *Palaeogeography, Palaeoclimatology, Palaeoecology* **377**, 110–124.
- Grousset, F.E., Parra, M., Bory, A., Martinez, P., Bertrand, P., Shimmield, G., Ellam, R.M.**, 1998. Saharan wind regimes traced by the Sr-Nd isotopic composition of subtropical Atlantic sediments: last glacial maximum vs today. *Quaternary Science Reviews* **17**, 395–409.
- Grousset, P., Labeyrie, L., Sinko, J.A., Cremer, M., Bond, G., Cortijo, E., Huon, S.**, 1993. Patterns of ice rafted detritus in the glacial North Atlantic (40–55°N). *Paleoclimatology* **8**, 175–192.
- Handiani, D., Paul, A., Prange, M., Merkel, U., Dupont, L., Zhang, X.**, 2013. Tropical vegetation response to Heinrich Event 1 as simulated with the UVic ESCM and CCSM3. *Climate of the Past* **9**, 1683–1696.
- Heinrich, H.**, 1988. Origin and consequences of cyclic ice rafting in the Northeast Atlantic Ocean during the past 130,000 years. *Quaternary Research* **29**, 142–152.
- Hemming, S.R.**, 2004. Heinrich events: massive late Pleistocene detritus layers of the North Atlantic and their global climate imprint. *Reviews of Geophysics* **42**,
- Holz, C., Stuut, J.B.W., Henrich, R.**, 2004. Terrigenous sedimentation processes along the continental margin off NW Africa: implications from grain-size analysis of seabed sediments. *Sedimentology* **51**, 1145–1154.

- Itambi, A.C., von Dobeneck, T., Mulitza, S., Bickert, T., Heslop, D.,** 2009. Millennial-scale northwest African droughts related to Heinrich events and Dansgaard-Oeschger cycles: evidence in marine sediments from offshore Senegal. *Paleoceanography* **24**, PA1205.
- Jaramillo-Vélez, A., Menéndez, I., Alonso, I., Mangas, J., Hernández-León, S.,** 2016. Grain size, morphometry and mineralogy of airborne input in the Canary basin: evidence of iron particle retention in the mixed layer. *Scientia Marina* **80**, 142–152.
- Jullien, E., Grousset, F., Malaizé, B., Duprat, J., Sanchez-Goñi, M.F., Eynaud, F., Charlier, K., Schneider, R., Bory A., Bout, V., et al.,** 2007. Low-latitude “dusty events” vs. high-latitude “icy Heinrich events.” *Quaternary Research* **68**, 379–386..
- Koopmann, B.,** 1981. Sedimentation von Saharastaub im subtropischen Nordatlantik während der letzten 25.000 Jahre. *Meteor Forsch Ergeb Reihe C* **35**, 23–59.
- McGee, D., DeMenocal, P.B., Winckler, G., Stuut, J.B., Bradtmiller, L.I.,** 2013. The magnitude, timing and abruptness of changes in North African dust deposition over the last 20,000 yr. *Earth and Planetary Science Letters* **371–372**, 163–176.
- McManus, J.F., Bond, G.C., Broecker, W.S., Johnsen, S., Labeyrie, L., Higgins, S.,** 1994. High-resolution climate records from the North Atlantic during the last interglacial. *Nature* **371**, 326–329.
- McManus, J.F., Oppo, D.W., Cullen J.L.,** 1999. A 0.5-Million-year record of millennial-scale climate variability in the North Atlantic. *Science* **283**, 971–975.
- Meco, J., Muhs, D.R., Fontugne, M., Ramos, A.N.J.G, Lomoschitz, A., Patterson, D.A.,** 2011. Late Pliocene and Quaternary eurasian locust infestations in the Canary Archipelago. *Lethaia* **44**, 440–454.
- Meco, J., Petit-Maire, N., Fontugne, M., Shimmield, G., Ramos, A.J.,** 1997. The Quaternary deposits of Lanzarote and Fuerteventura (Eastern Canary Islands, Spain): an overview. In *Climates of the past: proceedings of the CLIP meeting held june 2–7, 1995, Lanzarote and Fuerteventura / coord. por Nicole Petit-Maire; Joaquín Meco Cabrera (ed. lit.), 1997, págs. 123–136; ISBN 84-89728-18-6,*
- Menéndez, I., Díaz-Hernández, J.L., Mangas, J., Alonso, I., Sánchez-Soto, P.J.,** 2007. Airborne dust accumulation and soil development in the north-east sector of Gran Canaria (Canary Islands, Spain). *Journal of Arid Environments* **71**, 57–81.
- Menéndez, I., Pérez-Chacón, E., Mangas, J., Tauler, E., Engelbrecht, J.P., Derbyshire, E., Cana, L., Alonso, I.,** 2014. Dust deposits on La Graciosa Island (Canary Islands, Spain): texture, mineralogy and a case study of recent dust plume transport. *CATENA* **117**, 133–144.
- Middleton, J.L., Mukhopadhyay, S., Langmuir, C.H., McManus, J.F., Huybers, P.J.,** 2018. Millennial-scale variations in dustiness recorded in mid-Atlantic sediments from 0 to 70 ka. *Earth and Planetary Science Letters* **482**, 12–22.
- Mikolajewicz, U., Vizcaíno, M., Jungclaus, J., Schurgers, G.,** 2007. Effect of ice sheet interactions in anthropogenic climate change simulations. *Geophysical Research Letters* **34**,18.
- Moreno, A., Targarona, J., Henderiks, J., Canals, M., Freudenthal, T., Meggers, H.,** 2001. Orbital forcing of dust supply to the North Canary Basin over the last 250 kyr. *Quaternary Science Reviews* **20**, 1327–1339.
- Muhs, D.R., Budahn, J., Skipp, G., Prospero, J.M., Patterson, D.A., Bettis, E.A.,** 2010. Geochemical and mineralogical evidence for Sahara and Sahel dust additions to Quaternary soils on Lanzarote, eastern Canary Islands, Spain. *Terra Nova* **22**, 399–410.
- Mulitza, S., Prange, M., Stuut, J.B., Zabel, M., von Dobeneck, T., Itambi, A.C., Nizou, J., Schulz, M., Wefer, G.,** 2008. Sahel megadroughts triggered by glacial slowdowns of Atlantic meridional overturning. *Paleoceanography* **23**, 1–11.
- Naughton, F., Sánchez Goñi, M.F., Kageyama, M., Bard, E., Duprat, J., Cortijo, E., Desprat, S., Malaizé, B., Joly, C., Rostek, F., et al.,** 2009. Wet to dry climatic trend in north-western Iberia within Heinrich events. *Earth and Planetary Science Letters* **284**, 329–342.
- Ojanuga, A.G.,** 1979. Clay mineralogy of soils in the Nigerian tropical savanna regions. *Soil Science Society of America Journal* **43**, 1237–1242.
- Ortiz, J.E., Torres, T., Yanes, Y., Castillo, C., de la Nuez, J., Ibáñez, M., Alonso, M.R.,** 2006. Climatic cycles inferred from the aminostratigraphy and aminostratigraphy of Quaternary dunes and palaeosols from the eastern islands of the Canary Archipelago. *Journal of Quaternary Science* **21**, 287–306.
- Preusser, F.,** 2003. IRSL dating of K-rich feldspars using the SAR protocol: comparison with independent age control. *Ancient TL* **221**, 17–23.
- Prospero, J.M., Mayol-Bracero, O.L.,** 2013. Understanding the transport and impact of African dust on the Caribbean basin. *Bulletin of the American Meteorological Society* **94**, 1329–1337.
- Ravelo-Pérez, L., Rodríguez, S., Galindo, L., García, M.I., Alastuey, A., López-Solano, J.,** 2016. Soluble iron dust export in the

high altitude Saharan Air Layer. *Atmospheric Environment* **133**, 49–59.

**Rodrigues, T., Alonso-García, M., Hodell, D.A., Rufino, M., Naughton, F., Grimalt, J.O., Voelker, A.H.L., Abrantes, F.**, 2017. A 1-Ma record of sea surface temperature and extreme cooling events in the North Atlantic: a perspective from the Iberian margin. *Quaternary Science Reviews* **172**, 118–130.

**Roettig, C.B., Faust, D.**, 2018. Paleosurfaces separating dune generations of northern Fuerteventura. In: Geophysical Research Abstract EGU General Assembly. Vol. 20. EGU2018-16490, 2018

**Roettig, C.B., Kolb, T., Wolf, D., Baumgart, P., Richter, C., Schleicher, A., Zöller, L., Faust, D.**, 2017. Complexity of Quaternary aeolian dynamics (Canary Islands). *Palaeogeography, Palaeoclimatology, Palaeoecology* **472**, 146–162.

**Roettig, C.B., Kolb, T., Zöller, L., Zech, M., Faust, D.**, 2020. A detailed chrono-stratigraphical record of Canarian dune archives - interplay of sand supply and volcanism. *Journal of Arid Environments* **183**, 104240.

**Roettig, C.B., Varga, G., Sauer, D., Kolb, T., Wolf, D., Makowski, V., Espejo J.M.R., Zöller, L., Faust, D.**, 2019. Characteristics, nature, and formation of palaeosurfaces within dunes on Fuerteventura. *Quaternary Research* **91**, 4–23.

**Rother, H., Shulmeister, J., Rieser, U.**, 2010. Stratigraphy, optical dating chronology (IRSL) and depositional model of pre-LGM glacial deposits in the Hope Valley, New Zealand. *Quaternary Science Reviews*, Volume **29**, Issues 3–4, February 2010, Pages 576–592

**Ruddiman, W.F.**, 1977. Late Quaternary deposition of ice-rafted sand in the subpolar North Atlantic (lat 40° to 65°N). *Bulletin of the Geological Society of America* **88**, 1813–1827.

**Scheuvs, D., Schütz, L., Kandler, K., Ebert, M., Weinbruch, S.**, 2013. Bulk composition of northern African dust and its source sediments—a compilation. *Earth-Science Reviews* **116**, 170–194.

**Skonieczny, C., McGee, D., Winckler, G., Bory, A., Bradtmiller, L.I., Kinsley, C. W., Polissar, P.J., de Pol-Holz, R., Rossignol, L., Malaizé, B.**, 2019. Monsoon-driven Saharan dust variability over the past 240,000 years. *Science Advances*. **5**, 1–9.

**Stager, J.C., Ryves, D.B., Chase, B.M., Pausata, F.S.R.**, 2011. Catastrophic drought in the Afro-Asian monsoon region during Heinrich event 1. *Science* **331**, 1299–1302.

**Thiel, C., Buylaert, J-P., Murray, A., Terhorst, B., Hofer, I., Tsukamoto, S., Frechen, M.**, 2011. Luminescence dating of the Stratzing loess profile (Austria) – Testing the potential of an elevated temperature post-IR IRSL protocol. *Quaternary International* **234**, 23–31.

**Tjallingii, R., Claussen, M., Stuut, J.B.W., Fohlmeister, J., Jahn, A., Bickert, T., Lamy, F., Röhl, U.**, 2008. Coherent high- and low-latitude control of the northwest African hydrological balance. *Nature Geoscience* **1**, 670–675.

**Voelker, A.H.L., de Abreu, L.**, 2011. A Review of Abrupt Climate Change Events in the Northeastern Atlantic Ocean (Iberian Margin): Latitudinal, Longitudinal, and Vertical Gradients. In: **H. Rashid, L. Polyak, E. Mosley-Thompson** (Eds.), 2011. *Abrupt Climate Change: Mechanisms, Patterns, and Impacts*. Volume 193, 15–37. Geophysical Monograph Series

**Voelker, A.H.L., de Abreu, L., Schönfeld, J., Erlenkeuser, H., Abrantes, F.**, 2009. Hydrographic conditions along the western Iberian margin during marine isotope stage 2. *Geochemistry, Geophysics, Geosystems* **10**, Q12U08.

**von Suchodoletz, H., Faust, D., Zöller, L.**, 2009. Geomorphological investigations of sediment traps on Lanzarote (Canary Islands) as a key for the interpretation of a palaeoclimate archive off NW Africa. *Quaternary International* **196**, 44–56.

**von Suchodoletz, H., Fuchs, M., Zöller, L.**, 2008. Dating Saharan dust deposits on Lanzarote (Canary Islands) by luminescence dating techniques and their implication for palaeoclimate reconstruction of NW Africa. *Geochemistry, Geophysics, Geosystems* **9**, 1–19.

**von Suchodoletz, H., Oberhänsli, H., Faust, D., Fuchs, M., Blanchet, C., Goldhammer T., Zöller, L.**, 2009. The evolution of Saharan dust input on Lanzarote (Canary Islands) – influenced by human activity in the northwest Sahara during the early Holocene? *The Holocene* **20**, 2, 169–179.

**von Suchodoletz, H., Oberhänsli, H., Hambach, U., Zöller, L., Fuchs, M., Faust, D.**, 2010. Soil moisture fluctuations recorded in Saharan dust deposits on Lanzarote (Canary Islands) over the last 180 ka. *Quaternary Science Reviews* **29**, 2173–2184.

**von Suchodoletz, H., Zöller, L., Hilgers, A., Radtke, U., Faust, D.**, 2013. Vegas and dune-palaeosoil-sequences—two different palaeoenvironmental archives on the Eastern Canary Islands. In: **Fernández-Palacios, J.M., de Nascimento, L., Hernández, J.C., Clemente, S., González, A., Diaz-González, J.P.** (Eds.), *Climate Change Perspectives from the Atlantic: Past, Present and Future*. Servicio de Publicaciones, Universidad de La Laguna, pp. 259–274.

**Weinzierl, B., Ansmann, A., Prospero, J.M., Althausen, D., Benker, N., Chouza, F., Dollner, M., Farrell, D., Fomba, W.K., Freudenthaler, V., et al.**, 2017. The Saharan aerosol long-range transport and aerosol–cloud–interaction experiment: overview and selected highlights. *Bulletin of the American Meteorological Society* **98**, 1427–1451.

**Williams, R.H., McGee, D., Kinsley, C.W., Ridley, D.A., Hu, S., Fedorov, A., Tal, I., Murray, R.W., DeMenocal, P.B.**, 2016. Glacial to Holocene changes in trans-Atlantic Saharan dust transport and dust-climate feedbacks. *Science Advances*. **2**(11).

**Wintle, A.G.**, 1973. Anomalous fading of thermo-luminescence in mineral samples. *Nature* **245**, 143–144.

**Wintle, A.G., Murray, A.S.**, 2006. A review of quartz optically stimulated luminescence characteristics and their relevance in single-aliquot regeneration dating protocols. *Radiation Measurements* **41**, 369–391.

**Wright, A.K., Flower, B.P.**, 2002. Surface and deep ocean circulation in the subpolar North Atlantic during the mid-Pleistocene revolution. *Paleoceanography* **17**, 1068.

**Ziemen, F.A., Kapsch, M.L., Klockmann, M., Mikolajewicz, U.**, 2019. Heinrich events show two-stage climate response in transient glacial simulations. *Climate of the Past* **15**, 153–168.

**Ziemen, F.A., Rodehacke, C.B., Mikolajewicz, U.**, 2014. Coupled ice sheet–climate modeling under glacial and pre-industrial boundary conditions. *Climate of the Past* **10**, 1817–1836.

**Zöller, L., Pernicka, E.**, 1989. A note on overcounting in alpha-counters and its elimination. *Ancient TL* **7**, 11–14.

**Zou, Y., Boley, C.**, 2019. Eigenschaften und Klassifikation von Böden. In: **Boley C.** (Ed.). *Handbuch Geotechnik*. Springer Vieweg, Wiesbaden, pp. 13–57.

Loading [https://sonoisa.github.io/xyjax\\_ext/xy-pic.js](https://sonoisa.github.io/xyjax_ext/xy-pic.js)